

UC Irvine

UC Irvine Previously Published Works

Title

Performance evaluation of pulsed photothermal profiling of port wine stain in human skin

Permalink

<https://escholarship.org/uc/item/6958x2hq>

Journal

Review of Scientific Instruments, 75(6)

ISSN

0034-6748

Authors

Li, Bincheng
Majaron, Boris
Viator, John A
[et al.](#)

Publication Date

2004-06-01

DOI

10.1063/1.1753671

Copyright Information

This work is made available under the terms of a Creative Commons Attribution License, available at <https://creativecommons.org/licenses/by/4.0/>

Peer reviewed

Performance evaluation of pulsed photothermal profiling of port wine stain in human skin

Bincheng Li^{a)}

*Beckman Laser Institute and Medical Clinic, University of California at Irvine,
1002 Health Sciences Road East, Irvine, California 92612*

Boris Majaron

Jožef Stefan Institute, Jamova 39, SI-1000 Ljubljana, Slovenia

John A. Viator^{b)}

*Beckman Laser Institute and Medical Clinic, University of California at Irvine,
1002 Health Sciences Road East, Irvine, California 92612*

Thomas E. Milner

Biomedical Engineering Department, University of Texas, Austin, Texas 78712

J. Stuart Nelson

*Beckman Laser Institute and Medical Clinic, University of California at Irvine,
1002 Health Sciences Road East, Irvine, California 92612*

(Received 3 June 2003; accepted 29 March 2004; published online 24 May 2004)

Treatment of port wine stain (PWS) birthmarks in human skin by pulsed laser irradiation requires the knowledge of the maximum epidermal temperature rise and PWS depth for an attending physician to select the optimal light dosage, irradiation wavelength, and cryogen spray cooling spurt duration on an individual patient basis. Pulsed photothermal radiometry (PPTR) is a promising technique to provide such information. In this article, computer simulations are performed to evaluate the performance of PPTR depth profiling of the laser-induced temperature rise in PWS. An iterative, non-negatively constrained conjugate gradient algorithm is used to reconstruct the laser-induced temperature profile from simulated PPTR signals. Human skin is assumed to contain an epidermal melanin layer and a single homogeneous PWS layer in the dermis. The influence of structural, experimental, and algorithm parameters on the temperature profile reconstruction are discussed. Accuracy of the maximum epidermal temperature rise and PWS depth determined from the reconstructed profiles is statistically analyzed. The simulations show that when the melanin and PWS layers are physically discrete, a good reconstruction can be obtained and the maximum epidermal temperature rise and PWS depth can be determined with accuracy sufficient for the intended clinical application. Measurements and reconstructions from PWS patients are performed and the results are in agreement with the simulations. © 2004 American Institute of Physics.

[DOI: 10.1063/1.1753671]

I. INTRODUCTION

Port wine stain (PWS) is a congenital, progressive malformation of human skin.^{1–4} Histopathological studies of PWS show a normal epidermis overlying an abnormal plexus of dilated dermal blood vessels, as shown in Fig. 1. Epidermal melanin concentration, blood vessel size, distribution along the depth direction, etc., are important anatomical and physiological characteristics that vary on an individual patient basis, and even from site to site on the same patient. The pulsed laser can coagulate selectively PWS by inducing microthrombus formation within the targeted blood vessels.

The treatment of PWS by principle of selective photothermolysis⁵ (e.g., using a pulsed dye laser operating at 585–

595 nm) produces a complete fading of PWS only in a selected population of patients.⁶ We believe that this happens primarily because of the inability of the physician to select optimal treatment parameters on an individual patient basis. Selection of treatment parameters for each patient should be based on determination of: (1) maximum epidermal temperature rise immediately after laser irradiation due to melanin absorption; and (2) PWS depth. Knowledge of the maximum epidermal temperature rise allows the physician to determine the maximal light dosage for PWS destruction while avoiding epidermal damage. Knowledge of PWS depth is needed to determine the optimal irradiation wavelength and cryogen spray cooling (CSC) spurt duration applied prior to laser irradiation. CSC selectively cools and protects the epidermis from thermal damage^{7,8} and has increased the therapeutic efficacy of PWS laser treatment.^{8,9} However, in order to maximize the benefit of CSC, determination of the optimal spurt duration and delay between the spurt and laser pulse

^{a)}Present address: Institute of Optics and Electronics, Chinese Academy of Sciences, P.O. Box 350, Shuangliu, Chengdu, Sichuan 610209, China; electronic mail: belj@ioe.ac.cn

^{b)}Present address: Department of Dermatology, OP06, 3181 SW Sam Jackson Park Road, Oregon Health & Science University, Portland, OR 97239.

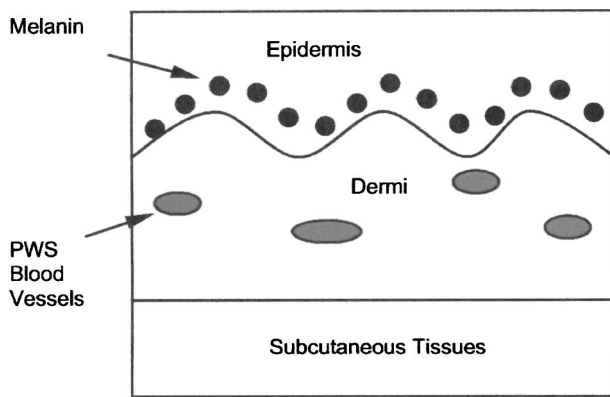


FIG. 1. Histopathology of human skin with PWS.

requires knowledge of both PWS depth and epidermal thickness.¹⁰

Pulsed photothermal radiometry (PPTR)^{11,12} is a noncontact method for obtaining information on the spatial distribution of the temperature rise in a substrate following pulsed laser irradiation. PPTR has been used to measure the subsurface temperature distribution in laser-heated PWS^{13–15} by measuring the temporal evolution of infrared (IR) emission from human skin. Using an inversion algorithm, PPTR signals are used to reconstruct the temperature distribution immediately after laser irradiation. From the reconstructed temperature profile, the maximum epidermal temperature increase, epidermal thickness, and PWS depth can be determined.^{13–15} Preliminary results^{13–18} have demonstrated that PPTR is a very promising tool for determination of PWS geometry in human skin and may eventually enable physicians to optimize PWS laser treatment on an individual patient basis.

One obstacle to clinical implementation of PPTR depth profiling is that the involved inverse problem is severely ill-posed,¹⁹ meaning that the reconstructed temperature profile is not unique, and is very sensitive to measurement noise. For reconstruction of the laser induced profile, an effective inverse algorithm and appropriate regularization strategy must be used.¹⁹ From previous research performed at our institution, we determined that an iterative, non-negatively constrained conjugate gradient inversion algorithm²⁰ with early termination regularization, is an effective method for reconstructing the laser-induced temperature rise in human skin PWS.^{14,15} While Sathyam and Prahl²¹ have reviewed

general limitations of PPTR profiling, and Smithies *et al.*²² discussed the limits on the position determination of a single discrete laser-heated subsurface chromophore, there has been no detailed analysis of PPTR on human skin containing both an epidermal melanin layer and subjacent PWS layer. Since epidermal melanin absorption is inevitably present in PWS skin and limits laser treatment efficacy, determination of both maximum epidermal temperature rise and PWS depth is important in clinical implementation of PPTR. The present study addresses the accuracy of maximum epidermal temperature rise and PWS depth determination using PPTR depth profiling in presence of an epidermal melanin layer.

Using computer simulations, we analyze the influence of structural, experimental, and algorithm parameters on PPTR temperature profile reconstruction. Specifically, the maximum epidermal temperature rise and PWS depth determined from the reconstructed profiles are statistically evaluated and compared to the simulation input values. The purpose of these simulations is to determine the optimal experimental parameters for practical measurements on PWS patients. Reconstruction of the temperature profiles from PWS patients is also presented and compared to the simulated results.

II. EXPERIMENTAL SETUP

The experimental setup designed for temperature profiling of laser-heated PWS skin was described in detail elsewhere^{15,17,23} and is schematically shown in Fig. 2. Briefly, pulsed laser radiation coupled into a 1 mm diameter multimode optical fiber is delivered onto the target after beam expansion by a handpiece and reflection by a microprism. IR emission from the target is collected by a lens and imaged onto a liquid nitrogen-cooled 256×256 InSb focal-plane-array camera (Galileo; Amber Engineering, Goleta, CA). To obtain a high acquisition rate (up to 1800 Hz) only a 64×64 pixel subwindow is used to record the IR emission in the 4.5–5 μm spectral range.²³ A sequence of 500 IR images is acquired in each measurement. For determination of temperature depth profile (averaged over a skin surface area of 1.9×1.9 mm²), each IR emission image is laterally averaged to yield a single radiometric signal value for that frame. The resulting time-dependent radiometric signal $\Delta S(t)$ is used as input for an inversion algorithm to reconstruct the depth resolved initial temperature rise following pulsed laser irradiation.

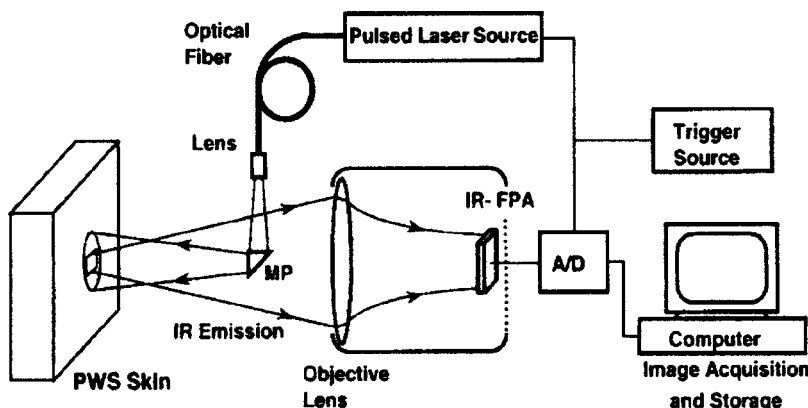


FIG. 2. Schematic diagram of experimental setup. MP: microprism. IR-FPA: Infrared focal plane array. A/D: analog-to-digital converter.

III. THEORY AND MODEL

The simulated skin model contains an epidermal melanin layer and a single homogeneous PWS layer in the dermis. Absorption of pulsed laser irradiation takes place in both layers due to the melanin in the epidermis and hemoglobin in blood vessels in the dermis. The laser spot diameter on the skin surface is assumed to be large relative to the thermal and optical diffusion lengths so that only one-dimensional thermal diffusion along the depth (z) axis is considered. Pulsed laser irradiation produces a temperature rise in the skin and, consequently, an increase in IR emission. The resulting PPTR signal is given by a Fredholm integral of the first kind¹⁴

$$\Delta S(t) = \int_z K(z,t) \Delta T(z,t=0) dz + n(t), \quad (1)$$

where $\Delta T(z,t=0)$ represents the temperature rise inside the skin immediately after pulsed laser irradiation and $K(z,t)$ is the kernel function. The noise term, $n(t)$, an inherent component in IR detection process, is taken as a zero-mean, Gaussian distributed function. The variance of the noise distribution is determined by the signal-to-noise ratio (SNR) of the PPTR signal:

$$\text{SNR} = \langle \Delta S(t) \rangle / \langle n^2(t) \rangle^{1/2}, \quad (2)$$

where $\langle \rangle$ represents time average.

The profile of the laser-induced temperature rise in PWS skin is determined by density, size, and spatial distribution of blood vessels in the dermis, as well as the effect of thermal diffusion during laser irradiation (typical pulse duration for PWS laser treatment is ~ 1 ms). Even though the laser-induced temperature profile may vary dramatically among PWS patients, no sharp edges would actually be present in the temperature profile, due to the combined effect of gradual onset of vascular network in PWS layer, lateral averaging over the 1.9×1.9 mm² skin area, and thermal diffusion during irradiation. In contrast with most earlier studies, which used discrete, box-like heated layers with unrealistic sharp edges,^{14,15,21,22} we therefore assume a hyper-Gaussian [n_1 in Eq. (3) is larger than 1] blood distribution in the PWS layer.^{4,23} We further assume that the temperature rise in the epidermal melanin layer has a hyper-Gaussian profile [n_2 in Eq. (4) is larger than 1]. The model temperature profile immediately after pulsed laser irradiation is, therefore

$$\begin{aligned} \Delta T(z,t=0) = & \Delta T_{01} \cdot \exp\left[-\left(\frac{z-z_{01}}{a_1}\right)^{2n_1}\right] \\ & + \Delta T_{02} \cdot \frac{\alpha(z)}{\alpha_0} \exp\left[-\int_0^z \alpha(z') dz'\right], \end{aligned} \quad (3)$$

with

$$\alpha(z) = \alpha_0 \cdot \exp\left[-\left(\frac{z-z_{02}}{a_2}\right)^{2n_2}\right]. \quad (4)$$

Here, ΔT_{01} and ΔT_{02} represent the maximum temperature rise in the epidermal and PWS layers, respectively, while a_1 , a_2 and z_{01} , z_{02} represent the thickness and central position of the epidermal melanin and PWS layers, respectively. Param-

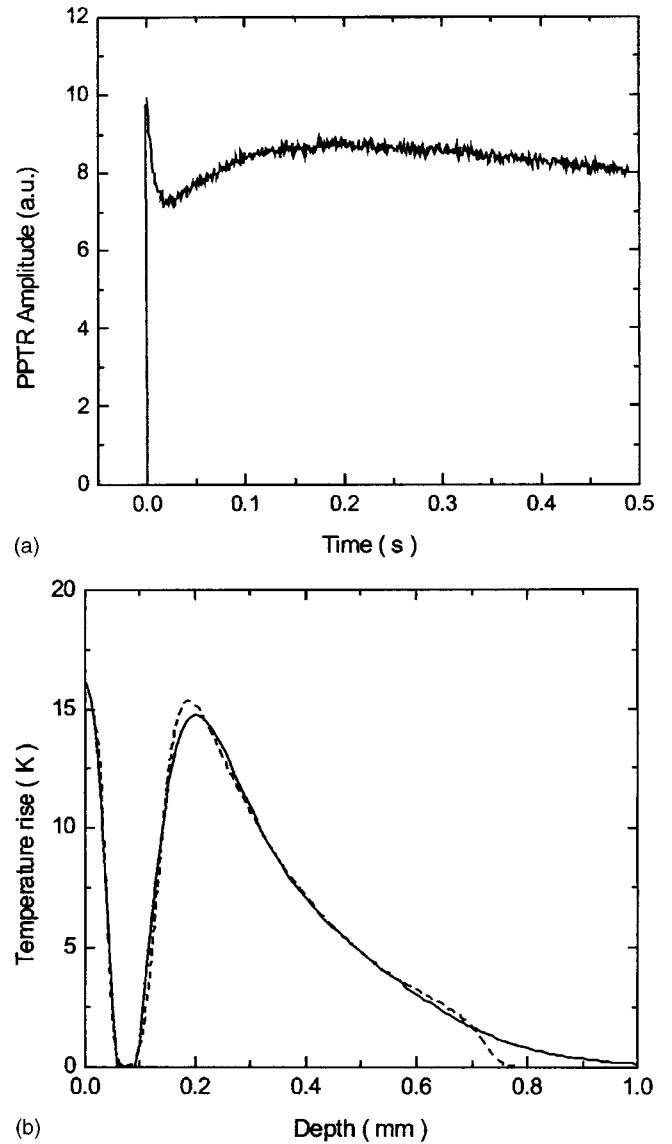
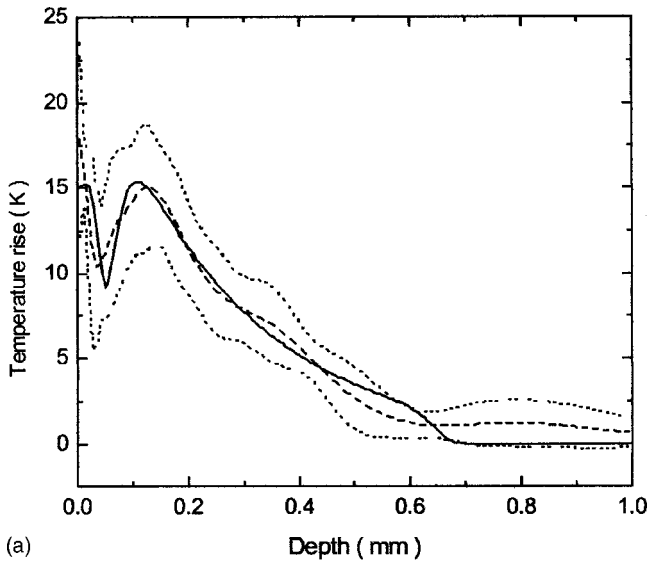


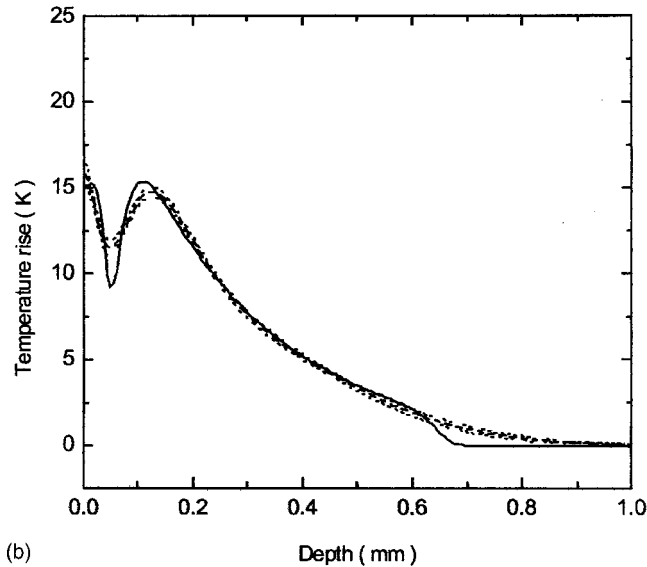
FIG. 3. Simulated temperature rise profile, corresponding PPTR signal, and reconstruction. (a) calculated PPTR signal with a SNR of 100; (b) simulated profile (dashed line) and a typical reconstruction (solid line) obtained with 100 iterations.

eters n_1 and n_2 define the profiles of the two layers and α_0 is the maximum absorption coefficient. By adjusting these parameters, various realistic temperature profiles inside PWS human skin can be simulated.

In the simulation, the PPTR signal is calculated by substituting the assumed initial temperature rise $\Delta T(z,t=0)$ into Eq. (1) and adding a random noise term $n(t)$ with variance determined by an assumed SNR value [Eq. (2)]. The PPTR signal is represented by 491 values at time points determined by the selected acquisition rate. Subsequently, the “noisy” PPTR signal is input into a non-negatively constrained conjugate gradient algorithm to reconstruct the initial temperature profile. In the reconstruction algorithm, the temperature rise in the most superficial 1.0–1.5 mm of skin (depending on PWS depth) is sought at 128 uniformly spaced nodes. If the reconstruction process develops instability, it is regularized by early termination using the L curve method.^{14,24} In this method, the Euclidean 2-norms of the reconstructed temperature profile $\|\Delta T^{(n)}\|$ is plotted versus



(a)



(b)

FIG. 4. Simulated (solid lines) and reconstructed (dashed lines) temperature profiles obtained with (a) 50, and (b) 5 iterations. Central position of the PWS layer is 0.35 mm and PWS layer partially overlaps the epidermal melanin layer. The reconstruction is repeated 25 times. Dashed line represents the mean profile and the two dotted lines represent the mean profile plus/minus standard deviation.

that of the residual vector $\|\Delta S - K\Delta T^{(n)}\|$ for increasing number of iterations (n). The iteration number that corresponds to the corner of the resulting curve, which often resembles the letter L (refer to Fig. 7 in Sec. V), is selected as optimal. If the reconstruction converges up to a large number of iterations, however, the process is terminated when the difference between the computed and simulated PPTR signals ceases to change between successive iterations, or at a pre-set number of iteration steps.

As an example, Fig. 3(a) shows a PPTR signal (frame rate 1000 Hz, noise term: SNR=100), corresponding to the model temperature profile represented by the dashed line in Fig. 3(b). The following parameter values are assumed in the simulation: $\Delta T_{01} = 15$ K, $\Delta T_{02} = 20$ K, $a_1 = 0.025$ mm, $a_2 = 0.3$ mm, $n_1 = 2$, $n_2 = 6$, $\alpha_0 = 4$ mm⁻¹, $z_{01} = 0$ mm, and $z_{02} = 0.43$ mm. Other parameters are: skin thermal diffusivity

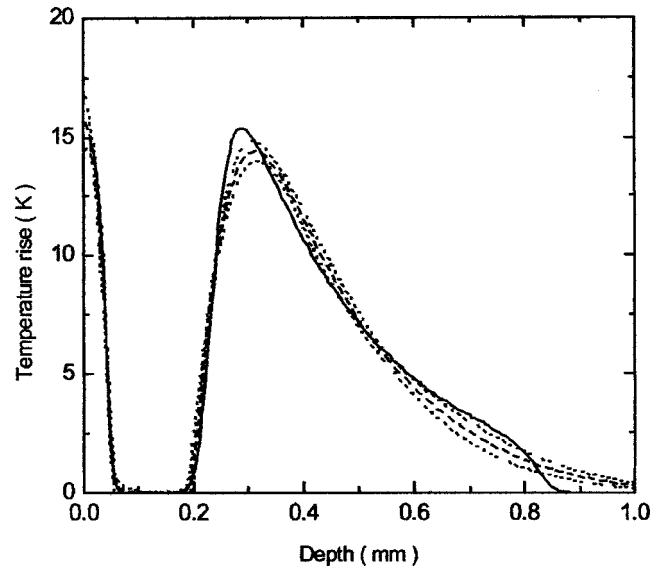


FIG. 5. Simulated (solid line) and reconstructed temperature profiles obtained with 150 iterations. The assumed PWS depth is approximately 0.2 mm. Dashed line represents the mean profile and the two dotted lines represent the mean profile plus/minus standard deviation.

$D = 0.11$ mm²/s, IR absorption coefficient of skin $\mu_{IR} = 26.5$ mm⁻¹,²³ and heat-loss coefficient at the skin/air interface $h = 0.03$ mm⁻¹.¹⁴ The reconstructed temperature rise obtained after 100 iteration steps is represented by the solid line in Fig. 3(b).

In the following section, we analyze the influence of various parameters on the temperature profile reconstruction and determination of the maximum epidermal temperature rise and PWS depth. Since the reconstruction process is sensitive to the specifics of random noise in the PPTR signal, the calculation is repeated 25 times for each simulated temperature profile, to allow statistical evaluation (mean reconstructed profile and standard variance) of the results.

IV. SIMULATION RESULTS

A. Influence of PWS depth

Since PWS depth varies on an individual patient basis,¹⁻⁴ we investigate how PWS depth affects the reconstruction. In the simulations, the parameter values used to compute the PPTR signal are the same as those used in Fig. 3, except for the central position of the PWS layer. The results show that the reconstruction is very sensitive to PWS depth. When the PWS layer is close to the heated epidermis, oscillation builds up in the reconstructed temperature profile at early stages of the iteration. Figure 4 shows an example where the epidermal melanin and PWS layers partially overlap (with $z_{02} = 0.35$ mm). The reconstructions averaged to obtain the mean profile presented in Fig. 4(a) are overiterated and unstable solutions, resulting in a large standard deviation. To prevent oscillation, the reconstruction process must be regularized. We apply the early termination approach and use the L curve technique to determine the optimal number of iterations.^{13,23} The profile shown in Fig. 4(b) was obtained with five iteration steps—an optimal number as determined

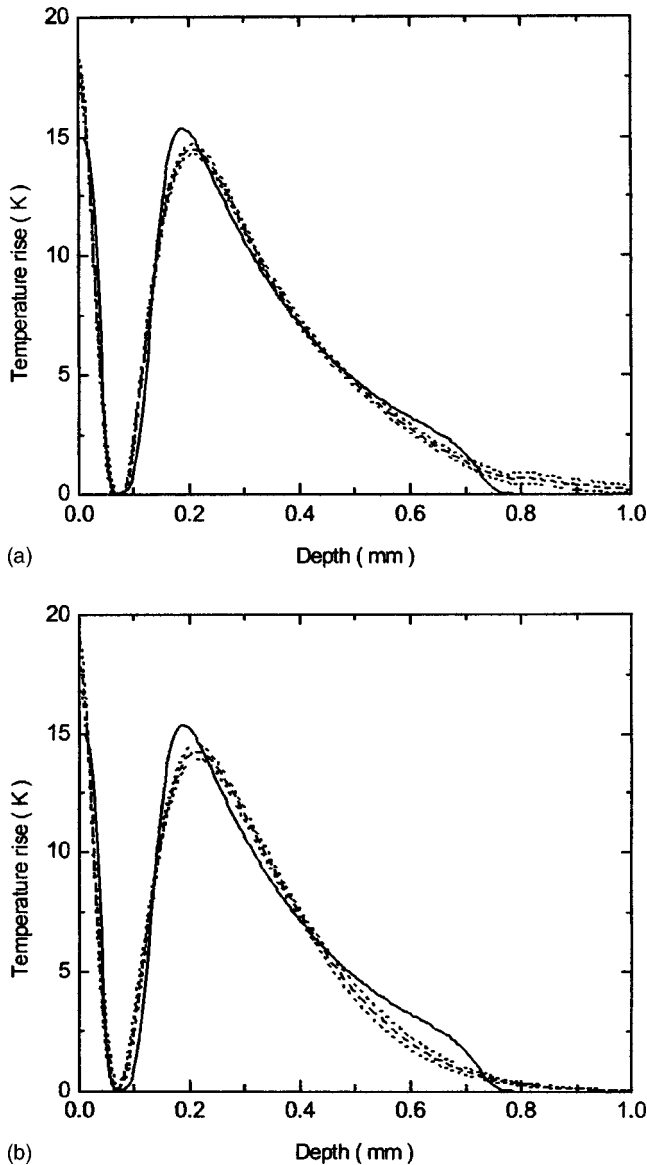


FIG. 6. Reconstruction of temperature profiles with noisy PPTR signals recorded at different frame rates. (a) Frame rate is 400 Hz and the SNR is 140. Number of iterations is 50; (b) Frame rate is 1500 Hz and the SNR is 70. Number of iterations is 6.

using the L curve method. Even though the standard deviation is much smaller, however, fine structures are still not resolved in the reconstructed profile.

When the PWS layer is located deeper in the skin, the magnitude of oscillation in the reconstruction becomes smaller and a better reconstruction can be obtained using more iteration steps. When the PWS depth (top boundary of the PWS layer) is greater than a characteristic depth, no apparent oscillation in the reconstruction occurs up to a rela-

tively large iteration number and the reconstruction converges toward the simulated profile. This characteristic depth is a complicated function of many structural and experimental parameters, such as PPTR signal SNR, magnitude of the epidermal temperature rise, epidermal melanin layer thickness, and PWS layer profile. According to the results of our simulation, the characteristic depth becomes deeper with decreasing SNR, increasing melanin layer temperature rise, larger epidermal melanin thickness, and sharper edge of the PWS layer. With the previous parameter values, the characteristic depth is approximately 0.1 mm. Provided that the top boundary of the PWS layer is deeper than 0.1 mm, a reconstruction can be obtained that is very close to the simulated profile. Figure 5 shows an example of the reconstruction with $z_{02}=0.53$ mm (PWS depth is approximately 0.2 mm). From the reconstructed temperature profile, clinically relevant lesion parameters, such as the maximum epidermal temperature rise and PWS depth, can be determined with adequate accuracy (refer to Sec. IV C).

B. Influence of acquisition rate

In theory, a high frame rate is preferable to resolve high-frequency components of the profile, especially in the superficial skin layer.²¹ Practically, however, higher frame rates often imply short acquisition periods, as the number of the PPTR signal data points may be limited by the data storage capacity of the IR imaging system or reconstruction computation time. Consequently, if the acquisition period is too short to record the signal contribution from deeper PWS layers, the result may be adversely affected.

Furthermore, high frame rates limit the integration times to collect the IR emission at each frame, which inevitably results in a reduced SNR level. For example, our IR camera has a data readout rate of 10^7 pixels per second, so the total readout time for the 64×64 pixel array is approximately 0.41 ms. The detector integration time, which must be shorter than the difference between the frame period and readout time is, therefore, limited to 0.25 ms at 1500 Hz, 0.5 ms at 1000 Hz, 1 ms at 700 Hz, and lower frame rates. (Integration times longer than 1 ms are usually not used to avoid detector saturation.) Several sources contribute to measurement noise in IR detection. For all prevalent noise contributions (Johnson, dark current and shot noise), however, SNR of the PPTR signal is proportional to the square root of the integration time.²⁵

Figure 6 shows the temperature profiles reconstructed with different frame rates, assuming the SNR is 140 at 400 Hz [Fig. 6(a)] and 70 at 1500 Hz [Fig. 6(b)], respectively. Theoretically, more details would be resolved using the higher frame rate. However, the associated reduction in SNR

TABLE I. Comparison of simulation results obtained with different SNR values in PPTR signals (number of iteration steps: $n=50$). Input values are: maximum epidermal temperature rise $\Delta T_{\text{EPI}}=15$ K, PWS depth ~ 103 μm .

SNR	50	100	200	400	1000
* ΔT_{EPI} (K)	17.7 ± 2.1	17.0 ± 1.2	17.3 ± 0.7	17.0 ± 0.6	17.5 ± 0.5
PWS depth (μm)	91.6 ± 6.2	90.6 ± 5.5	90.0 ± 3.1	91.6 ± 3.2	90.7 ± 2.8

TABLE II. Simulation results obtained with varying number of iteration steps (SNR=140).

Number of iterations	20	50	100	200	200 (SNR=280)
ΔT_{EPI} (K) (input value: 15 K)	17.8±0.4	17.2±0.8	16.6±1.0	16.5±1.4	16.3±0.8
PWS depth (μm) (input value: ~103 μm)	84.8±2.2	91.5±3.8	95.4±5.1	99.2±6.6	98.6±3.3

limits the optimal reconstruction to a lesser number of iteration steps. At 1500 Hz, the optimal number of iterations is 6 (as determined using the L curve technique), while no oscillations in the reconstructed profile occur up to a large number of iterations at 400 Hz. The mean reconstructed profile at 400 Hz [50 iteration steps; Fig. 6(a)] is thus closer to the simulated profile, and the standard deviation is also smaller.

C. Determination of maximum epidermal temperature rise and PWS depth

The clinical aim of the discussed PPTR depth profiling in human skin is to determine the maximum epidermal temperature rise (ΔT_{EPI}) and PWS depth. In this section, we present a statistical analysis of how structural, experimental, and algorithm parameters affect these results. To reduce the discretization error, the reconstructed profile is evaluated at 256 uniformly spaced nodes. The frame rate used is 700 Hz and the corresponding SNR is 140 unless specified otherwise. The remaining parameter values are the same as used in Fig. 3, except for the parameter varied in a particular test.

Table I presents the results obtained with varying SNR and a fixed number of iterations ($n = 50$). When the SNR is only 50, reconstruction is overiterated and partially oscillating. (Four highly oscillating reconstructions were excluded from the analysis because ΔT_{EPI} and PWS depth could not be determined.) The results show that increasing SNR from 50 to 200 decreases the standard deviation of ΔT_{EPI} and PWS depth by a factor of 3 and 2, respectively. No further significant improvement in the standard deviation is observed for either parameter above SNR=200. It is important to note, however, that the differences between the mean determined values and corresponding input values are not significantly reduced with increasing SNR.

Table II presents the results obtained with different numbers of iterations and a fixed SNR of 140. The mean values of both reconstructed parameters approach the input values as the number of iterations increases, but the standard deviations also increase. With 200 iterations, the reconstruction is overiterated and partially oscillating, resulting in relatively

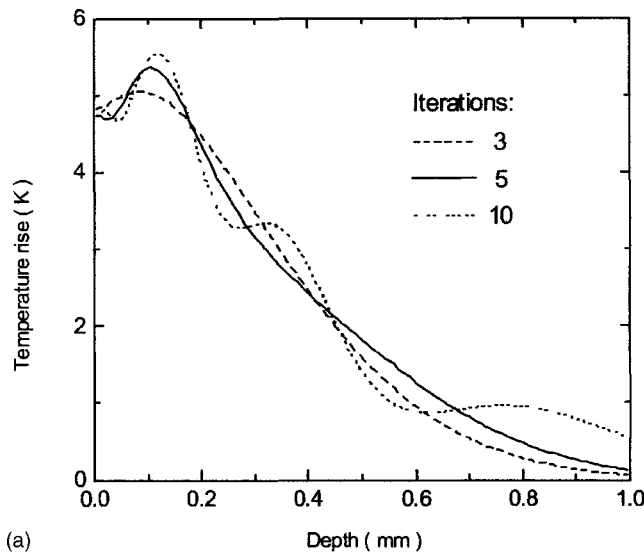
large standard deviations of ΔT_{EPI} and PWS depth. For determination of both parameters from a single PPTR signal, 50–100 iteration steps is thus optimal for the discussed example. However, if the SNR is improved by a factor of 2 (to 280), 200 iterations can be used with variances cut roughly in half. These results illustrate the importance of high SNR levels in the PPTR signals: a high SNR level permits the use of more iteration steps in the reconstruction process before the adverse effect of noise takes over, and thereby improves the accuracy of the reconstructed temperature profile.

Table III shows the influence of PWS depth. The reconstruction is terminated after 100 iteration steps. When the PWS layer depth is increased from 0.1 to 0.2 mm, the standard deviation of the maximum epidermal temperature rise decreases, indicating that more iteration steps could be used to further improve the mean value. For PWS depth determination, the relative error does not change significantly with input depth, and amounts to 6%–7%. The behavior of the standard deviation is similar to that of the epidermal temperature rise; decreasing for PWS depth up to 0.2 mm, and stalling thereafter. It is worthy of mention that the results presented in Table III are obtained using a constant SNR level. In reality, however, the SNR of the PPTR signal would decrease with increasing PWS depth, as the average PPTR signal amplitude decreases for PWS located deeper in the skin. When the PWS layer is in close proximity to or overlaps the epidermal melanin layer, determination of PWS depth becomes difficult. In such a case, a two-wavelength approach may be a more accurate method to determine PWS depth.^{26,27}

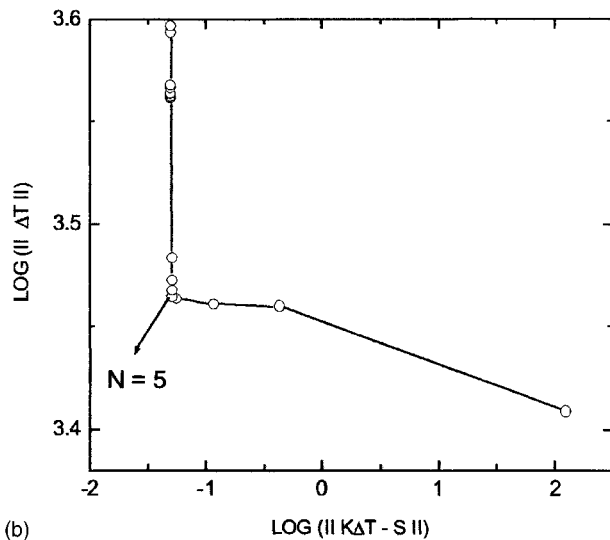
Accuracy of PWS depth determination is also influenced by the smoothness of the edges in the PWS temperature profile, determined by parameter n_2 in Eq. (4). Sharp edges cannot be resolved due to inherent bandwidth limitations of PPTR depth profiling. In accordance with previous studies, we found that the error in PWS depth determination increases with increasing n_2 value.

TABLE III. Statistical simulation results obtained with different PWS depths.

PWS Depth (μm) (input)	~103	~203	~303	~403
ΔT_{EPI} (K) (input value: 15 K)	16.6±1.0	16.6±0.5	16.0±0.5	16.3±0.5
PWS depth (μm) (reconstructed)	95.4±5.1	189.3±3.4	284.2±3.2	377.7±3.1
Mean reconstructed depth/input depth	0.926	0.933	0.938	0.937



(a)



(b)

FIG. 7. Temperature profile on a PWS site where PWS layer overlaps the epidermal melanin layer. (a) Reconstructions of the temperature rise with different numbers of iterations. (b) L curve indicates the optimal number of iterations is 5.

V. PWS PATIENT MEASUREMENTS

PPTR measurements were performed on several skin sites from one PWS patient. Figure 7 shows one reconstruction where the epidermal melanin and PWS layers are overlapping.²⁶ Figure 7(a) presents underiterated ($n=3$) to overiterated reconstructions ($n=10$). From Fig. 7(b), which presents the corresponding L curve, the optimal number of iterations is 5, determined from the corner of the L curve. Although the maximum epidermal temperature rise can be estimated from the reconstructed profile, PWS depth cannot be determined.

On another PWS test site, where blood vessels are deeper in the skin, well below the epidermal melanin layer, the reconstruction is very stable and the result insensitive to the number of iterations (Fig. 8). Both the maximum epidermal temperature rise and PWS depth can be determined accurately from the reconstruction. These experimental obser-

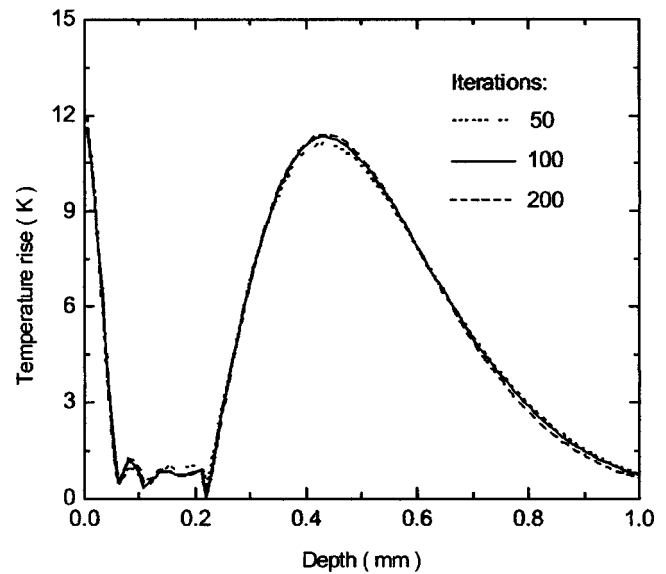


FIG. 8. Reconstruction of a PWS site where the epidermal melanin and PWS layers are well separated. The numbers of iterations are 50 (dotted line), 100 (solid line), and 200 (dashed line), respectively.

variations are in good agreement with the simulation results presented earlier.

VI. DISCUSSION

In summary, selection of the optimal acquisition rate depends primarily on noise level in the IR detection system and dimensions (and thermal diffusivity) of the sample. For optimal depth profile reconstructions, the frame rate must be high, providing the required spatial resolution, yet selected to yield PPTR signals with a suitably high SNR and acquisition periods long enough to detect the radiometric signal from deeper parts of the object. For the discussed experimental system, we find that the optimal frame rate for depth profiling in PWS human skin is around 700 Hz.

From the presented results, PPTR enables determination of PWS depth with an error of 6%–7% (which amounts to just 20 μm at PWS depth of 0.3 mm) when the epidermal and PWS temperature profiles do not overlap. Since the dependence of the optimal CSC spurt duration and laser pulse delay on PWS depth is quite weak,¹⁰ this error margin is clinically acceptable for selecting the optimal clinical parameters for PWS treatment. Another parameter affecting the selection of CSC parameters is epidermal thickness, which can also be determined from the same reconstructed profiles.¹⁰ The maximum epidermal temperature rise, which is determined with a lesser accuracy ($\sim 10\%$), on the other hand, serves mainly as an estimate of the maximal permissible irradiation dosage, but is not used directly in the determination of treatment parameters. Clinically, the maximal permissible dosage would usually not be applied in PWS treatment, as good acute response of the lesion can be achieved at significantly lower dosages.

It is worthy of mention that only random signal noise was considered in the simulations. In practice, many systematic errors can also contribute to inaccuracy of temperature profile determination. These sources include imperfect syn-

chronization of the IR camera with the laser pulse, uncertainty of skin thermal diffusivity, spectral variation of skin IR absorption coefficient, and errors in IR camera calibration. Care and effort must be taken to minimize these systematic errors to ensure accurate and reliable determination of clinically relevant characteristics of PWS lesions.

ACKNOWLEDGMENTS

The authors thank Guillermo Aguilar for helpful discussions. This work was supported by research grants from the National Institutes of Health Nos. (AR47551, AR48458, and GM62177), and Slovenian Ministry of Education and Science. Institutional support from the Office of Naval Research, Department of Energy, and the Beckman Laser Institute and Medical Clinic Endowment is also acknowledged.

- ¹S. H. Barsky, S. Rosen, D. E. Geer, and J. M. Noe, *J. Invest. Dermatol.* **74**, 154 (1980).
- ²O. T. Tan, P. Morrison, and A. K. Kurban, *Plast. Reconstr. Surg.* **86**, 1112 (1990).
- ³M. J. C. van Gemert *et al.*, *Phys. Med. Biol.* **42**, 937 (1997).
- ⁴D. J. Smithies, M. J. C. van Gemert, M. K. Hansen, T. E. Milner, and J. S. Nelson, *Phys. Med. Biol.* **42**, 1843 (1997).
- ⁵R. R. Anderson and J. A. Parrish, *Science* **220**, 524 (1983).
- ⁶C.-J. Chang, K. M. Kelly, M. J. C. van Gemert, and J. S. Nelson, *Lasers Surg. Med.* **31**, 352 (2002).
- ⁷J. S. Nelson, T. E. Milner, B. Anvari, B. S. Tanenbaum, S. Kimel, L. O. Svaasand, and S. L. Jacques, *Arch. Dermatol.* **131**, 695 (1995).
- ⁸B. Anvari, B. S. Tanenbaum, T. E. Milner, S. Kimel, L. O. Svaasand, and J. S. Nelson, *Phys. Med. Biol.* **40**, 1451 (1995).
- ⁹H. A. Waldorf, T. S. Alster, K. McMillan, A. N. Kauvar, R. G. Geronemus, and J. S. Nelson, *Dermatol. Surg.* **23**, 657 (1997).
- ¹⁰W. Verkruysse, B. Majaron, B. S. Tanenbaum, and J. S. Nelson, *Lasers Surg. Med.* **27**, 165 (2000).
- ¹¹A. C. Tam and B. Sullivan, *Appl. Phys. Lett.* **43**, 333 (1983).
- ¹²F. H. Long, R. R. Anderson, and T. F. Deutsch, *Appl. Phys. Lett.* **51**, 2076 (1987).
- ¹³S. L. Jacques, J. S. Nelson, W. H. Wright, and T. E. Milner, *Appl. Opt.* **32**, 2439 (1993).
- ¹⁴T. E. Milner, D. M. Goodman, B. S. Tanenbaum, and J. S. Nelson, *J. Opt. Soc. Am. A* **12**, 1479 (1995).
- ¹⁵T. E. Milner, D. J. Smithies, D. M. Goodman, A. Lau, and J. S. Nelson, *Appl. Opt.* **35**, 3379 (1996).
- ¹⁶T. E. Milner, D. M. Goodman, B. S. Tanenbaum, B. Anvari, L. O. Svaasand, and J. S. Nelson, *Phys. Med. Biol.* **41**, 31 (1996).
- ¹⁷S. A. Telenkov, B. S. Tanenbaum, D. M. Goodman, J. S. Nelson, and T. E. Milner, *IEEE J. Sel. Top. Quantum Electron.* **5**, 1193 (1999).
- ¹⁸S. A. Telenkov, D. J. Smithies, D. M. Goodman, B. S. Tanenbaum, J. S. Nelson, and T. E. Milner, *J. Biomed. Opt.* **3**, 391 (1998).
- ¹⁹P. C. Hansen, *Inverse Probl.* **8**, 849 (1992).
- ²⁰D. M. Goodman, E. M. Johansson, and T. W. Lawrence, in *Multivariate Analysis: Future Directions*, edited by C. R. Rao (North-Holland, Amsterdam, 1993).
- ²¹U. S. Sathyam and S. A. Pahl, *J. Biomed. Opt.* **2**, 251 (1997).
- ²²D. J. Smithies, T. E. Milner, B. S. Tanenbaum, D. M. Goodman, and J. S. Nelson, *Phys. Med. Biol.* **43**, 2453 (1998).
- ²³B. Majaron, W. Verkruysse, B. S. Tanenbaum, T. E. Milner, and J. S. Nelson, *Phys. Med. Biol.* **47**, 1929 (2002).
- ²⁴C. L. Lawson and R. J. Hanson, *Solving Least Squares Problems* (Prentice-Hall, Englewood Cliffs, NJ, 1974).
- ²⁵E. L. Dereniak and D. G. Crowe, *Optical Radiation Detectors* (Wiley, New York, 1984).
- ²⁶B. Majaron, W. Verkruysse, B. S. Tanenbaum, T. E. Milner, S. A. Telenkov, D. M. Goodman, and J. S. Nelson, *Phys. Med. Biol.* **45**, 1913 (2000).
- ²⁷B. Majaron, T. E. Milner, and J. S. Nelson, *Rev. Sci. Instrum.* **74**, 387 (2003).